International Journal of Automotive Technology, Vol. 18, No. 2, pp. 279−292 (2017)
DOI 10.1007/s12239−017−0028−2

pISSN 1229−9138/ eISSN 1976−3832

REAL-TIME WEIGHTED MULTI-OBJECTIVE MODEL PREDICTIVE CONTROLLER FOR ADAPTIVE CRUISE CONTROL SYSTEMS

R. C. ZHAO[1)], P. K. WONG[1)*], Z. C. XIE[2)] and J. ZHAO[1)]

[1)]Department of Electromechanical Engineering, University of Macau, Macau 999078, China
[2)]School of Mechanical and Automotive Engineering, South China University of Technology, 510641, China

(Received 2 March 2016; Revised 3 August 2016; Accepted 5 August 2016)

ABSTRACT−In this paper, a novel spacing control law is developed for vehicles with adaptive cruise control (ACC) systems to perform spacing control mode. Rather than establishing a steady-state following distance behind a newly encountered vehicle to avoid collision, the proposed spacing control law based on model predictive control (MPC) further considers fuel economy and ride comfort. Firstly, a hierarchical control architecture is utilized in which a lower controller compensates for nonlinear longitudinal vehicle dynamics and enables to track the desired acceleration. The upper controller based on the proposed spacing control law is designed to compute the desired acceleration to maintain the control objectives. Moreover, the control objectives are then formulated into the model predictive control problem using acceleration and jerk limits as constrains. Furthermore, due to the complex driving conditions during in the transitional state, the traditional model predictive control algorithm with constant weight matrix cannot meet the requirement of improvement in the fuel economy and ride comfort. Therefore, a real-time weight tuning strategy is proposed to solve time-varying multi-objective control problems, where the weight of each objective can be adjusted with respect to different operating conditions. In addition, simulation results demonstrate that the ACC system with the proposed real-time weighted MPC (RW-MPC) can provide better performance than that using constant weight MPC (CW-MPC) in terms of fuel economy and ride comfort.

KEY WORDS : Adaptive cruise control, Model predictive control, Real-time weight tuning, Fuel economy, Ride comfort

NOMENCLATURE

a_h : acceleration of host vehicle, m/s^2
a_{min} : minimum acceleration limit of host vehicle, m/s^2
a_{max} : maximum acceleration limit of host vehicle, m/s^2
a_p : acceleration of preceding vehicle, m/s^2
b : constrains of system for input and output
C_u : parameter matrix of constrains
d : relative distance between preceding and host vehicle, m
d_{des} : Desired relative distance, m
d_s : Safety distance, m
F : fuel consumption, grams
G : parameter matrix of cost function
H : parameter matrix of cost function
m : control horizon
p : prediction horizon
P : disturbance vector
R : set-point vector
$\boldsymbol{S}_x, I, \boldsymbol{S}_d, \boldsymbol{S}_u$: matrix parameter of predicted output performance vector
T_h : constant-time headway, s
u : control input
v_h : velocity of host vehicle, m/s
w_u : corresponding weight of input increment
w_d : corresponding weight of spacing error
w_v : corresponding weight of relative velocity error
w_a^k : corresponding weight of acceleration
Y_p : prediction performance vector
Γ_u : weight scale of input increment
Γ_y : weight matrix of output
Δd : errors of relative distance, m
ΔU : change of control vector
Δu : control input increment
Δv : errors of relative velocity, m/s
Δu_{min} : minimum incremental limit of control input, m/s^2
Δu_{max} : maximum incremental limit of control input, m/s^2
Δx : change of system state variable
$\Delta \rho$: change of system disturbance

*Corresponding author. e-mail: fstpkw@umac.mo

1. INTRODUCTION

Adaptive cruise control (ACC) is an extension of the traditional cruise control (CC), which is initially used to reduce the drivers' workload and improve convenience of drivers (Xiao and Gao, 2010; Santhanakrishnan and Rajamani, 2003; Lee *et al*., 2013). The existing ACC systems have been commercialized as a widespread functionality that can ensure the safety of host vehicle by keeping a desired spacing or tracking a desired velocity of a preceding vehicle. With the advances of electronic systems, more safety indexes, such as inter-distance, acceleration and ride comfort, have been imposed on the existing ACC systems. However, few investigations can be found in the open literature with respect to the development of the ACC system which considers the vehicle safety, ride comfort, fuel economy simultaneously. As a result, this paper focuses on the design and examination of a novel ACC system with consideration of vehicle safety, ride comfort, and fuel economy simultaneously.

To accomplish the aforesaid objectives in the ACC system, a proper control algorithm should be chosen first. There have been reported by many researches that the genetic algorithm (McGehee and Yoon, 2015), particle swarm optimization (Drehmer *et al*., 2015) and sliding mode control (Goggia *et al*., 2015), etc. are some common methods for settling the multi-objective control problem. However, it has been also proved that the model predictive control (MPC) method is also an effective way in solving the multi-objective control problem, particularly in the design of ACC systems (Li *et al*., 2011; Luo *et al*., 2010). The benefits of the MPC in the control of the multi-objective problem can be easily summarized as follows: (1) The multiple objectives can be formulated in a unified multi-variable framework of the MPC controller; (2) The constructed multi-variable system with MPC method can be easily accessed and adjusted by the designer; (3) The constraints of the multi-variable system that preset by the designer can be tuned within a wide range; (4) An online optimization can be performed; (5) The simplicity of the constructed multi-variable system can lead to a fast response with less computation time.

In this connection, some attempts have been done in applying the MPC method to the multi-objective control of vehicle ACC systems (Li *et al*., 2011; Luo *et al*., 2010). On this basis, a more explicit MPC method is developed based on a systematic approach. With this method, the key characteristics of the multivariable system can be parametrized to facilitate the control of the ACC system (Naus *et al*., 2010). Nevertheless, reference (Li *et al*., 2011; Naus *et al*., 2010) did not take the fuel economy into account in the design of ACC systems. To further decrease the fuel consumption influenced by ACC systems, an ecological vehicle driving system is built with safety concerns (Kamal *et al*., 2009). However, the construction of the vehicle fuel consumption model is based on the anticipation of future road-traffic situations, in which the nonlinear effects of vehicle longitudinal dynamics are not considered. In addition, a stochastic control strategy has been developed and examined in an ACC system with an improvement of 5 % fuel consumption (McDonough *et al*., 2013). The deficiency of this paper is that not all the real working conditions of the ACC system are considered, but only a preceding vehicle with a constant velocity. As a result, one objective of this work is to construct a more comprehensive vehicle model with fuel consumption for the ACC system, and apply the MPC method to the proposed ACC system with consideration of vehicle real working conditions.

In general, the functions of the ACC system are achieved in the longitudinal direction of the vehicle. So, the control action of the ACC system can be viewed as longitudinal control of the vehicle, and it can be performed with two basic modes, namely velocity control and spacing control (Rajamani, 2012). In the first case, a velocity is usually preset by the driver on a vehicle with ACC system (or called host vehicle). If there is no preceding vehicle in the same lane (which means no vehicle can be found in front of the host vehicle), the host vehicle will undergo the velocity control mode to maintain the preset velocity. On the contrary, when a preceding vehicle is detected by the ACC system of the host vehicle, the control mode of the host vehicle will then be switched to the spacing control mode to avoid a collision with the preceding vehicle (Li *et al*., 2011; Rajamani, 2012; Rajamani *et al*., 2000). The velocity control function of the ACC system is provided by a normal cruise control system. Since there is significant room for improvement on spacing control mode, this paper focuses on the investigation of the spacing control mode.

Regarding the spacing control mode, it comprises two states, which are transient state and steady state. In the transient state, the aim of the ACC system is to establish a specified inter-vehicle distance (SIVD) between the preceding vehicle and the host vehicle, and also determine when to switch from velocity control mode to spacing control mode. Afterwards, a corresponding predetermined control algorithm will then take effect so as to drive the host vehicle reaching the preset SIVD. This maneuver has been successfully implemented and referred as a transitional maneuver (TM) (Fancher and Bareket, 1994). On this basis, the procedure through which the ACC vehicle maintains the SIVD is regarded as steady state operation (Swaroop and Hedrick, 1996). During the steady state operation, the control algorithm also takes effect in the ACC system to maintain the preset SIVD regardless of the maneuvers of the preceding vehicle.

Though numerous investigations have proved that both the above control modes and maneuvers are acceptable in the design of the ACC system (Sheikholeslam and Desoer, 1993; Liang and Peng, 1999; Sun *et al*., 2004), it is still worth mentioning that the ACC system may not always be able to perform the steady state operation when the following situations are encountered: (1) The preceding vehicle begins to decelerate or suddenly stop; (2) A undesirable vehicle from another lane cuts in the lane that the host vehicle is staying at and keeps an uncertain position between the host vehicle and preceding vehicle (Connolly and Hedrick, 1999; Baghwar *et al*., 2004; Kato *et al*., 2002); (3) A cutting out occurs on the preceding vehicle, which means the preceding vehicle changes the running lane from the current one to another, resulting in the host vehicle losing its tracking target (Li *et al*., 2011; Martinez and Canudas-De-Wit, 2007). Under the above potential conditions, the ACC system of the host vehicle will probably turn back to the transient state control mode for safety concerns. Therefore, it has raised great challenges in the design of the ACC system when taking the complex driving conditions into account.

To address the above concerns, there exists some investigations on the operations of the transient state of the ACC system (Li *et al*., 2011, 2013). However, the numerical results from these studies demonstrate that the tracking capacity of the host vehicle is not good enough, especially under a critical transient working condition. Moreover, in order to obtain a better ACC performance, a restricted deceleration rate is selected for the host vehicle. The constraint on the vehicle deceleration rate may bring out a slow deceleration response to the host vehicle, and also makes the host vehicle unable to perform a large jerk operation when a necessary brake torque is needed for collision avoidance. Therefore, an optimal operation in the transient state is another research objective for the proposed ACC system.

A review of previous research on the transitional operation shows a kinematic relationship between range and range rate to illustrate the requirement of transitional operation (Fancher and Bareket, 1994). The kinematic relationship can be used to formulate an algorithm to establish a specified inter-vehicle distance. A two-vehicle system is developed to design a control law for the host vehicle to avoid a collision (Baghwar *et al*., 2004). However, the control law is designed to analyze the host vehicle response without considering the necessary dynamic effects, which is generated by the engine model, transmission model during gear shifting, and brake model during the braking manoeuvers. In Ali *et al*. (2013), an ACC system is designed to compensate the dynamic effects and track the desired acceleration commands. It has been observed that the host vehicle successfully avoids collision with the preceding vehicle, and establishes the desired SIVD with zero-range-rate. Similarly, an ACC system was designed by using nonlinear model predictive control algorithm to obtain the prediction of future reference trajectories corresponding to the desired speed and distance (Shakouri and Ordys, 2014; Shakouri *et al*., 2012). Although, their researches indicated that the host vehicle could successfully establish a SIVD and ensure the safety, its response needs to be investigated to meet the improvement of fuel economy and ride comfort. Hence, focusing on the design of the ACC system for a host vehicle under complex driving conditions, MPC algorithm is extended to develop a spacing control law, which should consider the relative importance of the multi-objectives in the MPC cost function during optimization. Additionally, the importance of the multi-objectives is determined by the influence of the inter-vehicle statement (Kim *et al*., 2010, 2012).

In this paper, a spacing control law in the upper controller is proposed to achieve control objectives during spacing control mode in an ACC system. The ACC system is introduced to perform transitional and steady operations by considering the nonlinear longitudinal dynamics of vehicles. Besides, to improve the fuel economy and ride comfort, a real-time weight tuning strategy is proposed, which is a function of the current inter-vehicle variables, such as inter-vehicle distance and relative velocity. This paper is organized as follows. In Section 2, the proposed control strategy of the ACC system is described. In Section 3, a vehicle-following model is developed based on the ACC system. In Section 4, based on the framework of MPC, a real-time weight tuning strategy is employed to solve time-varying multi-objective optimization problem, which is constructed to compute the spacing control command in which safety, fuel economy and ride comfort are considered concurrently. In Section 5, baseline scenarios of steady state operation and transitional operation are defined. For these scenarios, the simulated responses of the ACC system with the proposed spacing control algorithm using real-time weighted MPC and the spacing control algorithm using constant weight MPC are evaluated and compared. In Section 6, a conclusion is given.

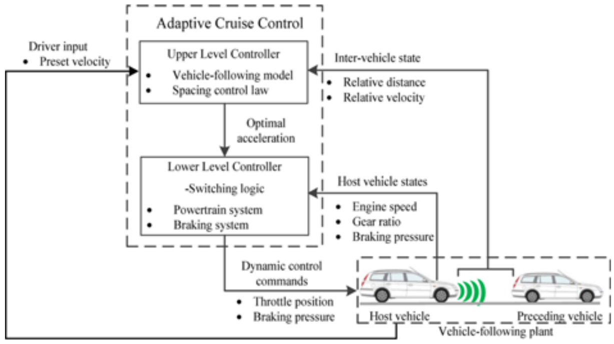

Figure 1. Hierarchical control structure of the proposed ACC system.

2. PROPOSED ACC SYSTEM

A hierarchical control structure is proposed to construct the controller of the ACC system, as shown Figure 1. The overall target of the hierarchical control strategy is to figure out the desired optimal acceleration and implement this optimal acceleration via a series of switching logics on the host vehicle to finally track the preceding the vehicle. The hierarchical structure is composed of two sub-controllers, which are the upper level controller and the lower level controller. The upper level controller, which includes the vehicle-following model and the spacing control law, is used to collect the inter-vehicle states and the driver input, and then computes an optimal acceleration for the host vehicle. The lower level controller is firstly used to collect the simultaneous state of the host vehicle, and then manipulates the powertrain system and braking system to achieve the best acceleration based on the switching logic.

In Figure 1, the function of ACC system is mainly achieved by the spacing control law contained in the upper level controller of the hierarchical structure. First of all, with the received inter-vehicle states (relative distance and/or relative velocity) and the driver input (preset velocity), the relationship of the vehicle following plant can be established through a vehicle-following model. Subsequently, an optimal acceleration can be computed via the spacing control law based on the established vehicle-following model, and then delivered as an input signal of the lower level controller.

In the lower level controller, there still exists a local control law, called switching logic, which is used to adjust the powertrain system and the braking system alternatively to achieve the desired optimal acceleration. With the application of the switching logic, the individual and alternative use of the powertrain system and the braking system can be realized, and then they are transformed into the throttle position and braking pressure of the host vehicle. In other words, by using the switching logic, the accelerator pedal and braking pedal of the vehicle can work individually and alternatively to achieve the desired optimized acceleration. Additionally, the instantaneous states of the host vehicle, such as engine speed, gear ratio and the braking pressure are also collected and sent to the lower level controller as feedback signals.

3. VEHICLE-FOLLOWING MODEL

To compute the best acceleration, the relationship of inter states between the host vehicle and the preceding vehicle should be established. The vehicle-following model is capable of reflecting the inter-vehicle states and thus constructed as the framework for the application of the spacing control law. Moreover, when applying the obtained throttle position signal and the braking pressure signal to the host vehicle, a time delay may probably be caused due to the response of the corresponding actuators, sensors, etc. To eliminate the time delay and manipulate the obtained signal timely, a first-order lag is employed in the construction of the vehicle-following model. The first-order lag has been proved to be effective in the compensation of the time delay of powertrain system and the braking system (Li *et al*., 2011; Rajamani *et al*., 2000), and it can be expressed as (Baghwar *et al*., 2004),

$$\tau \dot{a}_{\mathrm{h}}(t) + a_{\mathrm{h}}(t) = a_{\mathrm{des}}(t) \tag{1}$$

where τ refers to the first-order lag caused by the actuators and sensors during the implementation of the optimized acceleration.

The state variables of the vehicle-following model are the relative distance and relative velocity, which are also regarded as the inter-vehicle state between the host vehicle and the preceding vehicle. During the tracking process of the host vehicle, the inter-vehicle state is a variable, which means either the relative distance or the relative velocity changes over time. So, the error of relative distance and error of relative velocity can be respectively defined as,

$$\begin{cases} \Delta d(t) = d(t) - d_{\mathrm{des}}(t) \\ \Delta v(t) = v_{\mathrm{p}}(t) - v_{\mathrm{h}}(t) \end{cases} \tag{2}$$

where $d(t)$ is the relative distance between the preceding vehicle and the host vehicle, $d_{\mathrm{des}}(t)$ denotes desired relative distance preset through the ACC system, $v_{\mathrm{h}}(t)$ is the velocity of the host vehicle and $v_{\mathrm{p}}(t)$ is the velocity of the preceding vehicle. Moreover, $d_{\mathrm{des}}(t)$ can be calculated by the constant time-headway spacing policy, which can be formulated as,

$$d_{\mathrm{des}}(t) = T_{\mathrm{h}} v_{\mathrm{h}}(t) + d_0 \tag{3}$$

where d_0 is the safety distance. T_{h} is constant-time headway that can be figured out within the range of human reaction time 1.5 s ~ 2.5 s (2.5 s in this work).

Differentiating Equation (2) with respect to time, the following equation can be obtained,

$$\begin{cases} \Delta \dot{d}(t) = \Delta v(t) - T_{\mathrm{h}} a_{\mathrm{h}}(t) \\ \Delta \dot{v}(t) = a_{\mathrm{p}}(t) - a_{\mathrm{h}}(t) \end{cases} \tag{4}$$

According to Equation (1), the relationship between the desired acceleration and the host acceleration can be established, so the equation is equal to,

$$\dot{a}_{\mathrm{h}}(t) = \frac{1}{\tau} a_{\mathrm{des}}(t) - \frac{1}{\tau} a_{\mathrm{h}}(t) \tag{5}$$

By combining Equations (2) ~ (5), the dynamic equation of the system can be expressed as,

$$\begin{aligned} \dot{x}(t) = \begin{bmatrix} \Delta \dot{d}(t) \\ \Delta \dot{v}(t) \\ \dot{a}_{\mathrm{h}}(t) \end{bmatrix} &= \begin{bmatrix} 0 & 1 & -T_{\mathrm{h}} \\ 0 & 0 & -1 \\ 0 & 0 & -\frac{1}{\tau} \end{bmatrix} \begin{bmatrix} \Delta d(t) \\ \Delta v(t) \\ a_{\mathrm{h}}(t) \end{bmatrix} \\ &+ \begin{bmatrix} 0 \\ 0 \\ \frac{1}{\tau} \end{bmatrix} a_{\mathrm{des}}(t) + \begin{bmatrix} 0 \\ 1 \\ 0 \end{bmatrix} a_{\mathrm{p}}(t) \end{aligned} \tag{6}$$

More specifically, the vehicle-following model is a continuous-time system. In this connection, the vehicle-following model can be formulated as,

$$\begin{cases} \dot{x}(t) = \Phi x(t) + \Pi u(t) + \Omega \rho(t) \\ x(t) = \begin{bmatrix} \Delta d(t) & \Delta v(t) & a_{\mathrm{h}}(t) \end{bmatrix}^{\mathrm{T}} \\ u(t) = a_{\mathrm{des}}(t), \ \rho(t) = a_{\mathrm{p}}(t) \\ \Phi = \begin{bmatrix} 0 & 1 & -T_{\mathrm{h}} \\ 0 & 0 & -1 \\ 0 & 0 & -\frac{1}{\tau} \end{bmatrix}, \ \Pi = \begin{bmatrix} 0 \\ 0 \\ \frac{1}{\tau} \end{bmatrix}, \ \Omega = \begin{bmatrix} 0 \\ 1 \\ 0 \end{bmatrix} \end{cases} \tag{7}$$

where $x(t)$ is the system state, $u(t)$ is the control input, $\rho(t)$ is the system disturbance and $a_p(t)$ is the acceleration of the preceding vehicle.

In real-time control applications, the vehicle-following model is usually applied to the discrete-time domain, then it is converted into the discrete-time domain by zero-order hold (ZOH) discretization, expressing as,

$$\begin{cases} x(k+1) = Ax(k) + B_u u(k) + B_d \rho(k) \\ y(k) = Cx(k) \end{cases} \tag{8}$$

where k represents the k_{th} sampling time, A, B_u, B_d and C are system matrices, which can be expressed as,

$$A = \sum_{k=0}^{\infty} \frac{\Phi^k T_s^k}{k!},\ B_u = \sum_{k=0}^{\infty} \frac{\Phi^{k-1} T_s^k}{k!}\Pi,$$
$$B_d = \sum_{k=0}^{\infty} \frac{\Phi^{k-1} T_s^k}{k!}\Omega,\ C = \begin{bmatrix} 1 & 0 & 0 \\ 0 & 1 & 0 \\ 0 & 0 & 1 \end{bmatrix} \tag{9}$$

where T_s is sampling time (T_s = 100 ms), C is an identity matrix and $y \in R^3$ is the performance of vehicle-following system.

4. SPACING CONTROL LAW

This section describes the proposed spacing control law used for computing an optimal acceleration. The spacing control law is designed to solve the time-varying multi-objective MPC problem via the receding-horizon approach, in which the acceleration command computed at each sample time is a function of inter-vehicle states. Moreover, a real-time weight tuning strategy is also considered in the spacing control law to improve both fuel economy and ride comfort at the same time.

4.1. Control Objectives

Aiming to improve fuel economy and ride comfort of a driving action, the peak value of the longitudinal acceleration of the host vehicle a_h and the rate of change of longitudinal acceleration or deceleration j_h should be limited and minimized. Therefore, with the spacing control law, the targets of the ACC system can be considered as:

(1) The objective of vehicle-following behavior is that the ACC system regulates the host vehicle speed to that of the preceding vehicle to establish a desired SIVD.

$$Objective(A): \begin{cases} \Delta d(k) \to 0 \\ \Delta v(k) \to 0 \end{cases},\ as\ k \to \infty \tag{10}$$

(2) Fuel economy and ride comfort. When it is necessary to maintain a desired inter-vehicle distance, the host vehicle will accelerate and/or decelerate along with the movement of the preceding vehicle. For obtaining a better fuel economy and ride comfort, the proposed method is to decrease the values of acceleration and deceleration to avoid large acceleration $a_h(k)$ and jerk $j_h(k)$ (Ioannou and Xu, 1994; Yi and Kwon, 2001). With this method, another objective of the spacing control law can be expressed as,

$$Objective(B): \begin{cases} min|a_h(k)| \\ min|j_h(k)| \end{cases} \tag{11}$$

In order to implement a desired SIVD and acceptable fuel economy and ride comfort, some physical characteristics of the host vehicle should also be considered for the host vehicle in the vehicle-following model. At this point, it is also possible to apply the following constrains to the variables of the host vehicle.

$$\begin{cases} a_{min} \le a_h(k) \le a_{max} \\ j_{min} \le j(k) \le j_{max} \\ u_{min} \le u(k) \le u_{max} \end{cases} \tag{12}$$

where j_{min}, j_{max}, a_{min}, a_{max} are the bounds of jerk and acceleration, and the minimum and maximum values of $a_h(k)$ and $j(k)$ are defined with respect to the physical characteristic of the host vehicle. $u(k)$ is the control input that is calculated by the ACC system, and it should be also bounded according to the acceleration. All the parameters are constrained by the braking capacity and power capacity of the host vehicle, respectively.

(3) Safety concern. In the case of dangerous scenarios, such as the preceding vehicle takes an emergency braking, the host vehicle should always maintain a non-negative inter-vehicle clearance so that there is no rear-end collisions. The time-to-collision (TTC) strategy is used to restrain minimum distance. Together with minimum distance strategy, Equation (13) is designed to keep the host vehicle safe,

$$\begin{cases} d(k) \ge d_{safe}(k) \\ d_{safe}(k) = max\{TTC \cdot \Delta v(k), d_0\} \end{cases} \tag{13}$$

where $d_{safe}(k)$ refers to the safety threshold at the sample time k.

4.2. Optimal Model Predictive Control for ACC System

The function of the proposed ACC system is to compute the dynamic control commands and subsequently manipulates the host vehicle to a specified inter-vehicle distance, as well as meeting the demand of ride comfort

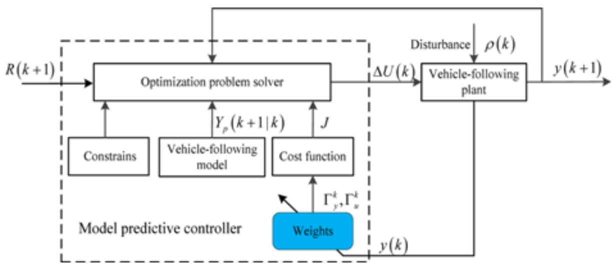

Figure 2. Schematic block diagram of the proposed MPC algorithm.

and fuel economy. This function is achieved with the spacing control law and can be formulated as an optimized MPC problem. The schematic block diagram of the MPC algorithm is shown in Figure 2.

During the transitional state, the reference is $R(k+1)$ described as control objective (A), the disturbance is the acceleration of the preceding vehicle $\rho(k)$. The output is $y(k+1)$, which are the relative distance error, the relative velocity error and the acceleration of host vehicle. A model predictive controller is designed to determine the dynamic control commands as control input vector $\Delta U(k)$ to meet the requirement of control objective (A). In the proposed model predictive controller, there are three parts including of constrains, vehicle-following model and cost function. The vehicle-following model is designed as Equation (7). A cost function is developed that considers low fuel consumption and ride comfort. Physical driving characteristics and safety are formulated as linear constrains described in Equations (12) and (13).

The basic principle of MPC is that the current control action is obtained by solving an optimization problem, and the value of the solved incremental control signal $\Delta U(k)$ is firstly applied. Then the discrete time horizon moves one step ahead, and the process is repeated. The future system states $Y_p(k+1|k)$ are predicted based on the model and the current state $x(k)$. Therefore, the incremental equation of the vehicle-following model is represented as,

$$\begin{cases} \Delta x(k+1) = A\Delta x(k) + B_u \Delta u(k) + B_d \Delta\rho(k) \\ y(k) = C\Delta x(k) + y(k-1) \end{cases} \tag{14}$$

where the change of system state is $\Delta x(k) = x(k) - x(k-1)$, the change of control input is $\Delta u(k) = u(k) - u(k-1)$, the change of system disturbance is $\Delta\rho(k) = \rho(k) - \rho(k-1)$. The predicted performance vector $Y_p(k+1|k)$ and the change of control input vector $\Delta U(k)$ of the ACC system at the sample time k are calculated as,

$$\begin{cases} Y_p(k+1|k) = \begin{bmatrix} y_p(k+1|k) \\ y_p(k+2|k) \\ \vdots \\ y_p(k+p|k) \end{bmatrix}_{p\times 1} \\ \Delta U(k) = \begin{bmatrix} \Delta u(k) \\ \Delta u(k+1) \\ \vdots \\ \Delta u(k+m-1) \end{bmatrix}_{m\times 1} \end{cases} \tag{15}$$

where p is the predicted horizon, m is the control horizon, $y_p(k+1|k), y_p(k+2|k),\ldots, y_p(k+p|k)$ are the predictive performance at the sample time k, $\Delta u(k)$, $\Delta u(k+1),\ldots$, $\Delta u(k+m-1)$ are the change of command sequence of the control signal. The predicted output performance vector is,

$$Y_p(k+1|k) = \boldsymbol{S}_x \Delta x(k) + \boldsymbol{I} y(k) + \boldsymbol{S}_d \Delta d(k) + \boldsymbol{S}_u \Delta U(k) \tag{16}$$

where $\boldsymbol{S}_x$, $\boldsymbol{I}$, $\boldsymbol{S}_d$ and $\boldsymbol{S}_u$ are the matrix parameters described in Appendix.

At the sample time k, the current disturbance (the acceleration of the preceding vehicle) $\rho(k)$ is immeasurable, but it can be approximated via the value of the previous sampling time $k-1$. The relationship between the current disturbance and its previous state can be expressed as,

$$\rho(k) = \rho(k-1|k) \tag{17}$$

where $\rho(k-1|k)$ is the disturbance of sampling time estimated at the sampling time $k-1$. Assuming that the disturbance remains constant in the prediction horizon, which is a common way of modeling the disturbance vector.

$$\rho(k+i) = \rho(k), i = 1,\ 2, \ldots, p-1 \tag{18}$$

Then, the disturbance vector $P(k)$ is obtained,

$$P(k) = \begin{bmatrix} \rho(k-1|k) \\ \rho(k-1|k) \\ \vdots \\ \rho(k-1|k) \end{bmatrix}_{p\times 1} \tag{19}$$

To calculate the optimal control input based on the performance of the vehicle-following plant, the following performance index is required to be minimized in the MPC.

$$\begin{aligned} &J\left(x(k), \Delta U(k)\right) \\ &= \left\|\Gamma_y Y_p(k+1|k) - R(k+1)\right\|^2 + \left\|\Gamma_u \Delta U(k)\right\|^2 \end{aligned} \tag{20}$$

where $R(k+1)$ is the set-point vectors associated with each output vector at the sample time $k+1$, Γ_u is the weight scale of input increment, Γ_y is the weight matrix of output. Combining Equations (16) and (20), and defining

$E_p(k+1|k) = R(k+1) - \boldsymbol{S}_x \Delta x(k) - \boldsymbol{I} y_c(k) - \boldsymbol{S}_d \Delta\rho(k)$,

the cost function can be then described as,

$$\begin{aligned} &\min J\left(x(k), \Delta U(k)\right) \\ &= \left\|\Gamma_y\left(\boldsymbol{S}_u \Delta U(k) - E_p(k+1|k)\right)\right\|^2 + \left\|\Gamma_u \Delta U(k)\right\|^2 \\ &= \Delta U(k)^T \boldsymbol{S}_u{}^T \Gamma_y{}^T \Gamma_y \boldsymbol{S}_u \Delta U(k) + \Delta U(k)^T \Gamma_y{}^T \Gamma_y \Delta U(k) \\ &\quad -2E_p(k+1|k)^T \Gamma_y{}^T \Gamma_y \boldsymbol{S}_u \Delta U(k) \\ &\quad +E_p(k+1|k)^T \Gamma_y{}^T \Gamma_y E_p(k+1|k) \end{aligned} \tag{21}$$

The ideal goal of Equation (21) is to simultaneously improve the ride comfort and minimize both average jerk level and total fuel consumption during the transitional maneuver. The optimized MPC is numerically calculated using a quadratic programming algorithm, so the cost function in Equation (21) is formulated based on the standard form of quadratic programming, $\Delta U(k)^T \boldsymbol{H} \Delta U(k) - \boldsymbol{g}^T \Delta U(k)$, then the following cost function is obtained.

$$\begin{cases} J = \Delta U(k)^T H \Delta U(k) - G(k+1|k)^T \Delta U(k) \\ Subject\ to, C_u \Delta U(k) \geq b(k+1|k) \end{cases}, \tag{22}$$

where $G(k+1|k)=2\boldsymbol{S}_u^{T}\Gamma_y^{T}\Gamma_y E_p(k+1|k)$ and $H = \boldsymbol{S}_u^{T}\Gamma_y^{T}\Gamma_y\boldsymbol{S}_u + \Gamma_u^{T}\Gamma_u$ are the parameter matrix of the cost function. It is noted that the last term $E_p(k+1|k)^{T}\Gamma_y^{T}\Gamma_y E_p(k+1|k)$ in Equation (21) is independent of $\Delta U(k)$, and it does not affect the calculation of $\Delta U(k)$ in quadratic programming. Therefore, $E_p(k+1|k)^{T}\Gamma_y^{T}\Gamma_y E_p(k+1|k)$ can be ignored in Equation (22). In Equation (22), C_u and $b(k+1|k)$ are the parameter of constrains described in Appendix. Γ_u and Γ_y are the weights of control input and output that can be described as,

$$\begin{cases} \Gamma_y = diag(\Gamma_{y,i}, \Gamma_{y,i}, \ldots, \Gamma_{y,i})_{p\times p} \\ \Gamma_u = diag(\Gamma_{u,i}, \Gamma_{u,i}, \ldots, \Gamma_{u,i})_{m\times m} \end{cases} \tag{23}$$

Meanwhile, in the cost function, the weights make a different performance for the ACC system. Assuming that at the sample time k, $\Gamma_{y,i}$ and $\Gamma_{u,i}$ are described as,

$$\Gamma_{y,i} = \Gamma_y(k) = \begin{bmatrix} w_d(k) & 0 & 0 \\ 0 & w_v(k) & 0 \\ 0 & 0 & w_a(k) \end{bmatrix} \tag{24}$$
$$\Gamma_{u,i} = \Gamma_u(k) = w_u(k)$$

where $w_d(k)$ is the corresponding weight of inter vehicle distance error $\Delta d(k)$, $w_v(k)$ is the corresponding weight of the relative velocity error $\Delta v(k)$, and $w_a(k)$ is the corresponding weight of acceleration $a_h(k)$. The weights $w_d(k)$, $w_v(k)$ and $w_a(k)$ are usually tuned by the designer so that users can select appropriate optimization objectives. Figure 3 shows the simulation results with three different sets of constant weight parameters given as,

$$\begin{cases} w_d = 1, w_v = 1, w_a = 1, w_u = 1 \\ w_d = 1, w_v = 1, w_a = 10, w_u = 1\,, \\ w_d = 1, w_v = 1, w_a = 20, w_u = 1 \end{cases} \tag{25}$$

Table 1. Parameters of the two vehicles for simulation.

Parameter	Value	Parameter	Value
v_{min}	0 m/s	u_{min}	– 0.25 g
v_{max}	36 m/s	u_{max}	0.5 g
a_{min}	– 0.5 g	Δu_{min}	– 4 m/s^3
a_{max}	0.5 g	Δu_{max}	2 m/s^3
Δj_{min}	– 4 m/s^3	T_s	100 ms
Δj_{max}	2 m/s^3	d_s	8 m
p	10	TTC	– 2.5 s
m	5	g	9.8 m/s^2
$w_d(0)$	10	$w_v(0)$	10
$w_a(0)$	1	$w_u(0)$	1

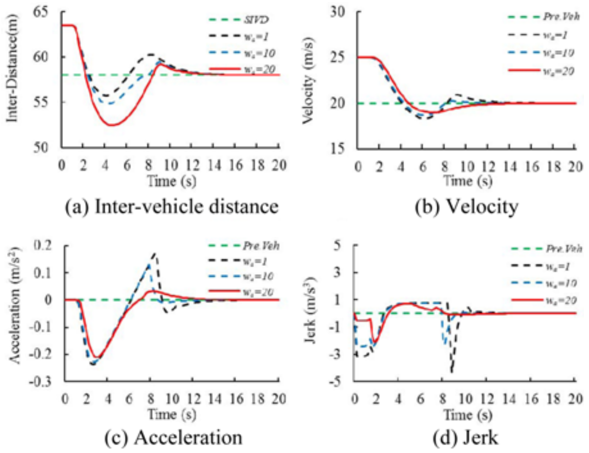

Figure 3. Host vehicle response to a negative cut-in with three different constant weights.

The simulation describes the case when a new preceding vehicle cuts in, and the relative parameters of the two vehicles for simulation are shown in Table 1.

The host vehicle is driving with a velocity v_h = 25 m/s corresponding to a negative cut-in at the beginning, the preceding vehicle shows up to 64 m in front of the host vehicle with a velocity v_p = 20 m/s. The host vehicle initially decelerates to prevent collision with the new preceding vehicle and then accelerates to track the desired inter-vehicle distance with the preceding vehicle as shown in Figures 3 (a) and (b). However, the velocity overshoot are undesired. To prevent these, the acceleration should be penalized more and the simulation results show that the negative velocity error and velocity overshoot are reduced as is tuned to increase.

However, if $w_d(k)$ is increased, the response of the closed loop system gets slower. Slow response can make the driver uncomfortable. Another solution is to increase w_v. In that case, when the inter-vehicle distance error is positive, the feedback term of the velocity error is positive and the acceleration can be reduced. However, when a new preceding vehicle cuts in and the velocity error is negative, the large w_v can cause undesirable system behavior. Therefore, during the complex vehicle-following scenarios, adjusting only one constant weight in the cost function cannot satisfy the desired control objectives. To control the motion of the host vehicle smoothly and prevent velocity overshoot, state dependent weights are suggested.

4.3. Real-time Weight Tuning Strategy

As shown in above section, MPC with constant weights hardly obtains satisfactory control performance for different complex situations in ACC systems. Therefore, a real-time weight tuning strategy is proposed to cope with the problem, while preventing the large velocity overshoot and maintaining a fast response and safety. There are three situations being considered in this study and they are shown below:

Table 2. Desired performance and weights.

Sign of error	$\Delta d < 0$ $\Delta v < 0$	$\Delta d < 0$ $\Delta v > 0$	$\Delta d > 0$ $\Delta v < 0$
Desired performance	Decelerate rapidly	Accelerate/ decelerate smoothly	Decelerate smoothly
Desire w_d	Large	Large	Small
Desire w_v	Large	Small	Large
Desired w_a	Small	Large	Large

(1) When both the inter-vehicle distance error and the relative velocity are negative ($\Delta d < 0, \Delta v < 0$, negative cut in), it is a dangerous situation and it is desirable to decelerate the host vehicle quickly. In that case, both the inter-vehicle distance error and the relative velocity should be more penalized while the acceleration should be less penalized to ensure a fast response.

(2) When the inter-vehicle distance error is negative $\Delta d < 0$ and the velocity error is positive $\Delta v > 0$, which describes the case when a preceding vehicle faster than the host vehicle cuts in, the host vehicle should smoothly accelerate or decelerate to keep the desired inter-vehicle distance with the new preceding one. The inter-vehicle distance error should be more penalized than the relative velocity, and the acceleration is more penalized to make a smooth motion to prevent the undesired overshooting.

(3) When the inter-vehicle distance error is positive $\Delta d >$ 0 and the relative velocity $\Delta v < 0$ is negative, it is desirable to maintain the speed to prevent an excessive velocity overshoot. Therefore, the inter-vehicle distance error should be less penalized while the relative velocity and the acceleration should be more penalized.

The desired performance of the host vehicle and corresponding weights for these three situations are described in Table 2.

Based on the aforesaid expert knowledge during the TMs, the real-time weight tuning function are suggested as follows,

$$\begin{cases} w_d(k) = \dfrac{1 - N(\Delta d(k-1))}{\gamma(k)} w_d(0) \\ w_v(k) = \dfrac{1 - N(\Delta v(k-1))}{\gamma(k)} w_v(0) \\ w_a(k) = \dfrac{1 - N(\Delta d(k-1)) \cdot N(\Delta v(k-1))}{\gamma(k)} w_a(0) \end{cases} \tag{26}$$

where

$$N(.) = \frac{2}{\pi} \tan^{-1}(.)$$

$$\begin{aligned} \gamma(k) = &\left[1 - N(\Delta d(k-1))\right] w_d(0) \\ &+ \left[1 - N(\Delta v(k-1))\right] w_v(0) \\ &+ \left[1 - N(\Delta d(k-1)) \cdot N(\Delta v(k-1))\right] w_a(0) \end{aligned}$$

In Equation (23), $w_d(k)$, $w_v(k)$, $w_a(k)$ are the weights for the inter-vehicle distance $\Delta d(k)$, the relative velocity $\Delta v(k)$, and the host vehicle acceleration at the sample time k, respectively, and they are designed to be adjusted with respect to the inter-vehicle states $\Delta d(k)$ and $\Delta v(k)$. Based on the suggested tuning strategy and the idea of fraction, when $\Delta d(k) < 0$ & $\Delta v(k) < 0$, $w_d(k)$ and $w_v(k)$ are tuned to increase, and $w_a(k)$ is tuned to decrease, and when $\Delta d(k) <$ 0 & $\Delta d(k) > 0$, $w_d(k)$ and $w_v(k)$ are tuned to increase, and $w_a(k)$ is tuned to decrease, and when $\Delta d(k) > 0$ & $\Delta d(k) < 0$, $w_v(k)$ and $w_a(k)$ are tuned to increase, and $w_d(k)$ is tuned to decrease. In the design of weight strategy for multi-objective MPC, the aforementioned situations in Table 2 can be achieved by using the initial weights. It can also be noticed that, with the normalization function $N(\cdot)$, $\Delta d(k)$ and $\Delta v(k)$ are transformed from $(-\infty, +\infty)$ to $(-1, 1)$. Using $\gamma(k)$, the weights are combined together and the sum of their adjustment coefficients is 1. With this suggested weight-tuning strategy, the above optimization problem can be rapidly solved to obtain an optimal control input, which is utilized as the control command to meet the requirement of vehicle safety, ride comfort, and fuel economy simultaneously.

It has to be noted that, although there are four weights (w_d, w_v, w_a and w_u) in the control system, only three weights (w_d, w_v and w_a) is considered in the weight tuning strategy. This is because from a set of trial-and-error simulations, it is found that a fixed value of w_u is good enough to frequently guarantee a fast response of the proposed controller. Therefore, no real-time adjustment is necessary for this weight. Besides, for the initial values of the weights $w_d(0)$, $w_v(0)$, $w_a(0)$ and $w_u(0)$, they are chosen through many trial-and-error simulations by considering the host vehicle safety, ride comfort, fuel economy simultaneously, and the values are given in Table 1.

5. SIMULATION AND DISCUSSION

In this section, the objective is to evaluate the performance of the proposed spacing control law for the ACC system. A set of general scenarios are determined to evaluate the performance of the controller as shown in Table 3. Based on this set of scenarios, a test program is setup as shown in Figure 4. Two ACC controllers are simulated and compared, one is the proposed MPC with real-time weighted strategy (RW-MPC), which is state dependent, and the other is MPC with constant weights (CW-MPC). The spacing control laws based on both CW-MPC and RW-MPC were implemented using MATLAB/Simulink and Carsim.

The simulation was carried based on the parameters in Table 1 and the sampling rate is 100 Hz. The simulation results of general situations of Table 3 for the two ACC controllers are presented below. For comparison of CW-MPC and RW-MPC performance, the results are indicated from Figure 5 to Figure 8.

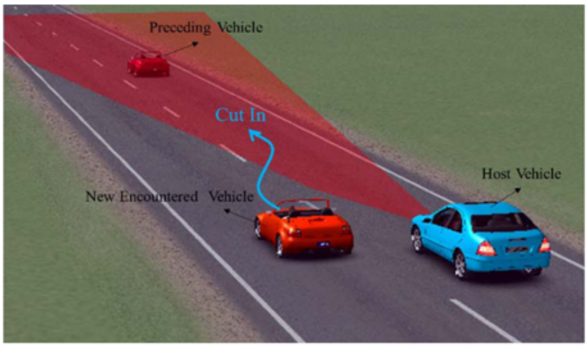

(a) Cut in scenario

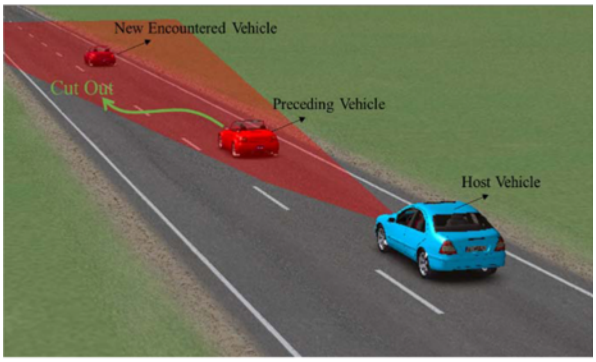

(b) Cut out scenario

Figure 4. Description of simulation scenarios.

Table 3. Desired performance and weights.

Case A:	A negative cut in, which involves a sudden step in Δd such that $\Delta d < 0$ and $\Delta v < 0$.
Case B:	A positive cut in, which involves a sudden step in Δd such that $\Delta d < 0$ and $\Delta v > 0$.
Case C:	A cut out, which involves a sudden step in Δd such that $\Delta d > 0$ and $\Delta v < 0$.
Case D:	An emergency, which involves a hardly deceleration.

5.1. Case A: Preceding Vehicle with Negative Cut-in Scenario.

In case of a negative cut in, it is assumed that the host vehicle is driving with a velocity v_h = 25 m/s, and a preceding vehicle (*Pre.Veh*) with velocity v_p = 20 m/s cuts in from another lane 65 m in front of the host vehicle. According to the vehicle following model Equation (7), the inter-vehicle distance error Δd is − 7 m, and the relative velocity between the two vehicles Δv is – 5 m/s.

In case of a negative cut in, a fast response of direct reaction and substantial braking are required from a safety point of view as described in Table 3. In Figure 5 (a), regarding safety point of view, both CW-MPC and RW-MPC can keep a safe inter-vehicle distance to prevent collision by substantial braking, and then the inter-vehicle distance converges to the final desired inter-vehicle distance. Because of an initial inter-vehicle distance error and the relative velocity are negative shown in Figures 5 (a) and (b), according to the real-time weighted strategy described in Equation (26), the weights of inter-vehicle distance w_d and the relative velocity w_v should be big, and the weight of acceleration w_a should be small as shown in Figure 5 (d). Therefore, the RW-MPC calculates an optimal control command which leads to smaller acceleration than that in CW-MPC as shown in Figure 5 (c). It prevents the velocity of host vehicle equipped with RW-MPC from overshooting. Accordingly, when a preceding vehicle is detected, the host vehicles equipped with CW-MPC and RW-MPC takes braking as a fast response and adjusts the throttle position to establish a zero-range-rate at the point of SIVD as indicated in Figures 5 (e) and (f).

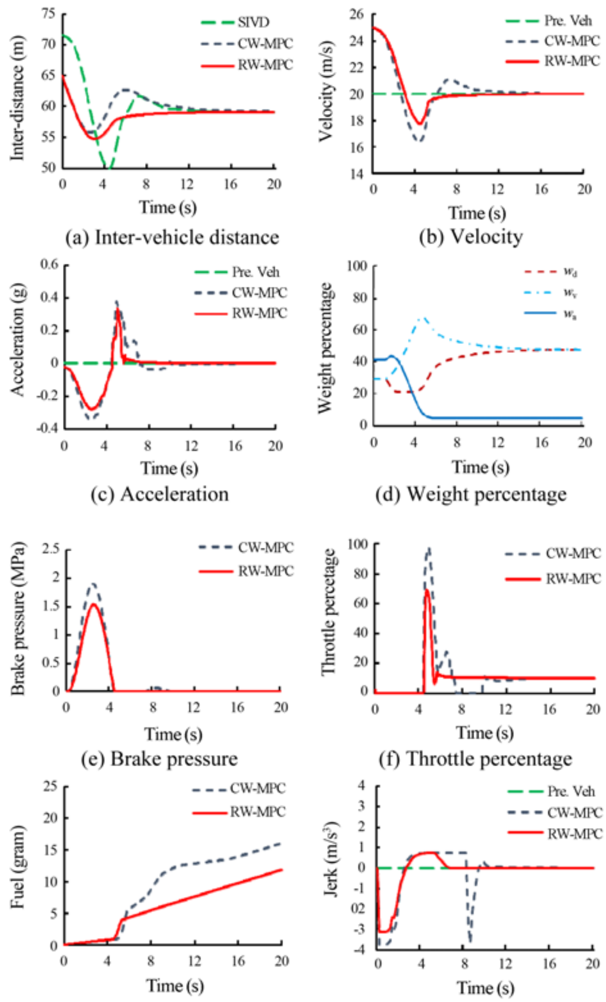

(a) Inter-vehicle distance (b) Velocity (c) Acceleration (d) Weight percentage (e) Brake pressure (f) Throttle percentage (g) Fuel consumption (h) Jerk

Figure 5. Host vehicle response to a negative cut-in.

5.2. Case B: Preceding Vehicle with Positive Cut-in Scenario

The host vehicle is driving with a velocity v_h = 20 m/s corresponding to a positive cut-in. A vehicle with velocity v_p = 25 m/s cuts in from another lane 52 m in front of the

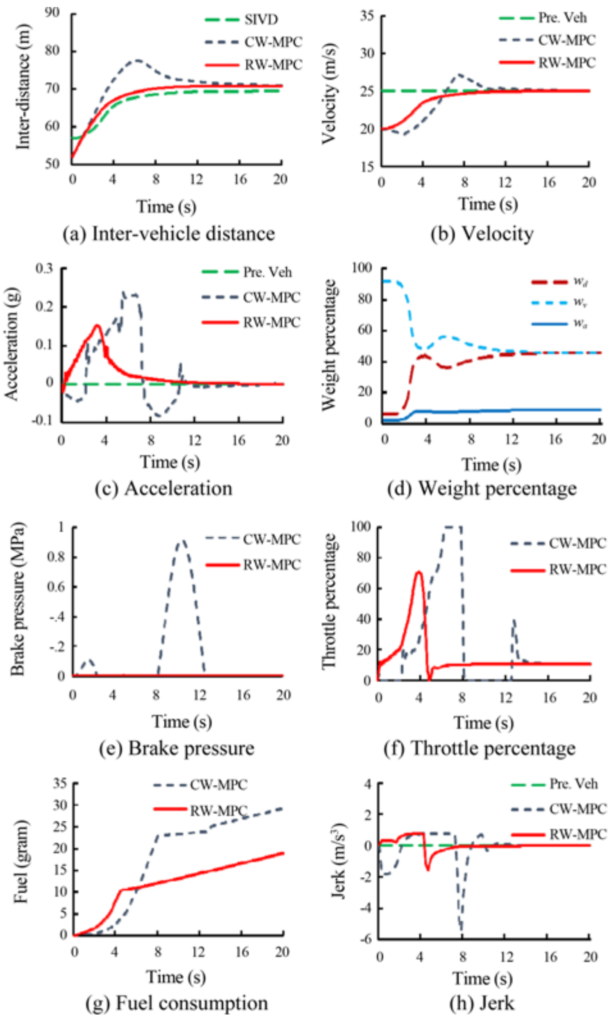

Figure 6. Host vehicle response to a positive cut-in.

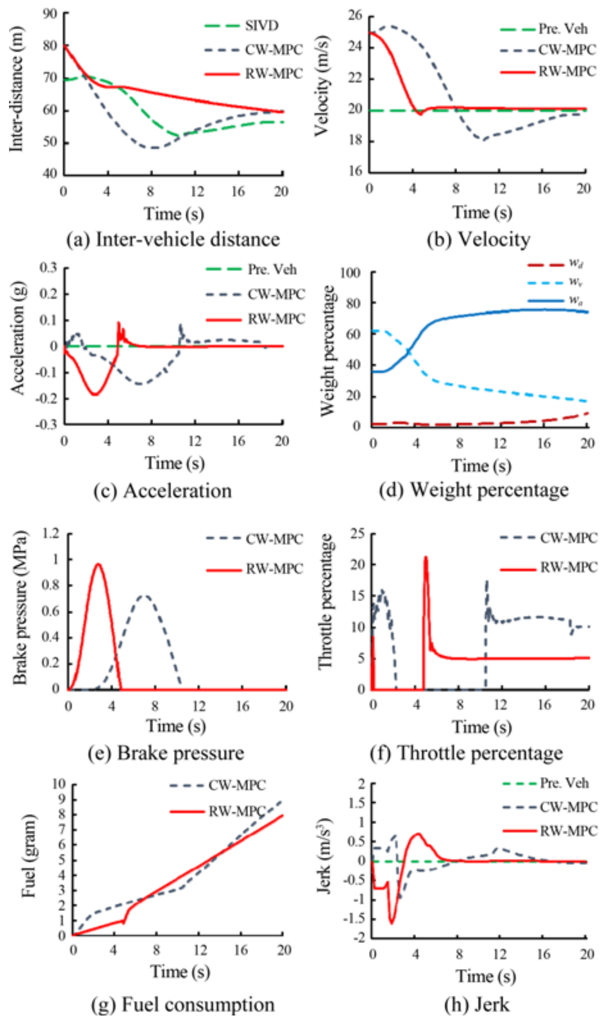

Figure 7. Host vehicle response to a cut-out.

host vehicle. According to the Equation (7), the inter-vehicle distance error Δd is – 6 m, and the relative velocity between the two vehicles Δv is 5 m/s.

In case of a positive cut in, a smooth acceleration is required from the control objective point of view. In Figure 6 (a) shown, both CW-MPC and RW-MPC can approach the desired inter-vehicle distance. Because of the negative inter-vehicle distance error and positive relative velocity error, based on the real-time weighted strategy described in Equation (26), the weights of the relative velocity should be decreased, and the weights of inter-vehicle distance error and acceleration should be increased as shown in Figure 6 (d). Therefore, it prevents the velocity of host vehicle equipped with RW-MPC from overshooting during the TM. Accordingly, when a preceding vehicle is detected, the host vehicles equipped with RW-MPC takes smaller acceleration.

5.3. Case C: Preceding Vehicle with Negative Cut-in Scenario

The host vehicle is driving with a velocity v_h = 25 m/s corresponding to cut-out. A new preceding vehicle with velocity v_p = 20 m/s is detected in the same lane 80 m in front of the host vehicle. According to Equation (7), the inter-vehicle distance error Δd is 12 m, and the relative velocity between the two vehicles Δv is – 5 m/s.

In case of a cut out as shown in Figure 7 (a), to prevent frequent cut-in from adjacent lanes, both CW-MPC and RW-MPC can approach the desired inter-vehicle distance finally. Because of the positive inter-vehicle distance error and relative velocity error, based on the real-time weighted strategy described in Equation (26), the weight of tracking the relative velocity error should be decreased, and the weights of the inter-vehicle distance error and acceleration should be increased as shown in Figure (d). Therefore, RW-MPC takes a smooth deceleration, and so it prevents the velocity of host vehicle from overshooting during the TM. However, though CW-MPC keeps a small acceleration, the velocity of the host vehicle continues to decrease as shown in Figures 7 (b) and (c). This leads to an undesirable overshooting of the host velocity and more fuel consumption. Accordingly, when a preceding vehicle is detected, the host vehicles equipped with RW-MPC takes a smooth acceleration to establish a safe inter-vehicle distance and avoids a collision with the preceding vehicle. The host vehicle based on the proposed spacing control law could adjust the throttle position to make the velocity converge to the velocity of the preceding vehicle, as shown Figures 7 (e) and (f).

5.4. Case D: Preceding Vehicle with Negative Cut-in Scenario

The host vehicle is driving with a velocity v_h = 20 m/s. A preceding vehicle appears in the same lane 57 m in front of the host vehicle. The preceding vehicle takes emergency braking. In this case of emergency, a fast response of direct reaction and substantial braking are required form a safety point of view. In Figure 8 (a), regarding safety point of view, the host vehicle with RW-MPC can keep a safe inter-vehicle vehicle distance to prevent collision by a higher

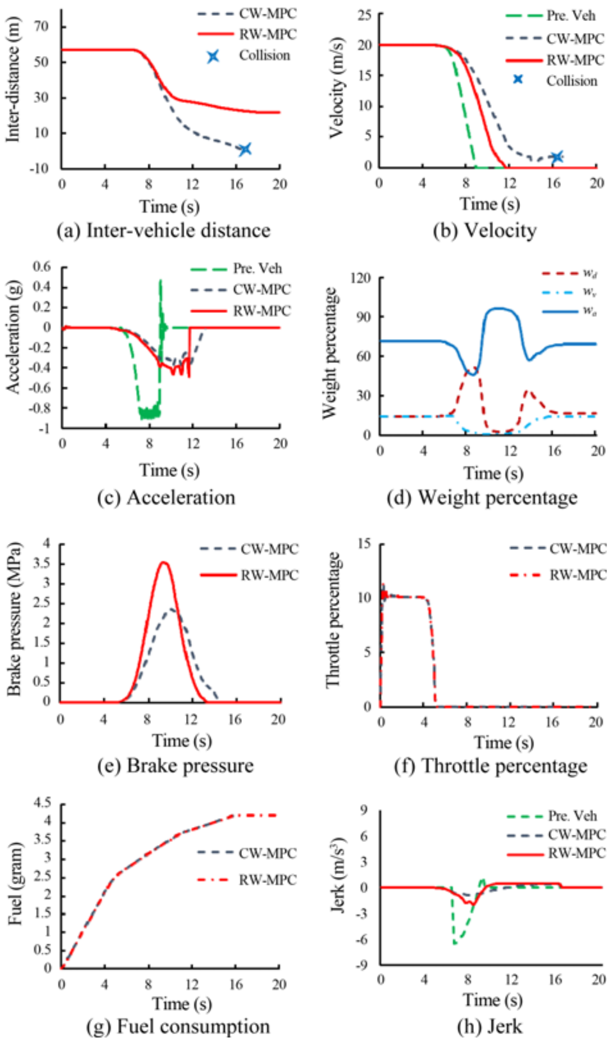

Figure 8. Host vehicle response to critical TM.

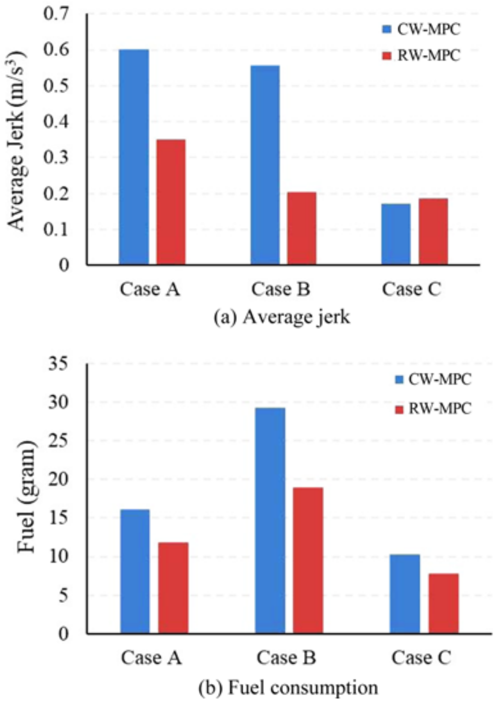

Figure 9. Comparison of simulation results in average jerk and fuel consumption.

deceleration. However, the host vehicle with CW-MPC have a traffic accident at the time t = 18 s as shown in Figure 8 shown. Based on the real-time weighted strategy described in Equation (26), at t = 6 s, the weight of inter-vehicle distance shifts to bigger values, and the weight of acceleration and velocity shifts to smaller values as shown in Figure 8 (d).

5.5. Overall Evaluation of Ride Comfort and Fuel Economy

The simulation results of the fuel economy and ride comfort are calculated by using Carsim based on a model of a conventional passenger car (B-Class, 4WD, AT). Compared with CW-MPC, most of the average jerk and fuel consumption in the RW-MPC are improved as shown in Figure 9. In Case A scenario, the average jerk value is reduced by 41.78 %, while the fuel consumption value decreases by 26.02 %. In Case B scenario, the average jerk value is reduced by 63.26 %, while the fuel consumption value decreases by 35.35 %. In Case C scenario, due to the compromise among a fast response, ride comfort and fuel economy, the fuel consumption value decreases by 23.7 %, but the average jerk value of RW-MPC is increased by 5.49 %. All the simulation results are shown in Table 4.

Tables 4 and 5 reveal that the spacing control law based on RW-MPC is superior to that based on CW-MPC in term of ride comfort and fuel economy. Especially in cut-in cases, both average jerk and fuel consumption can be decreased by a large margin. Bold indicates better performance.

Table 4. Comparison of ride comfort of CW-MPC and RW-MPC.

Case study	j_h (m/s^3)		Improvement
	CW-MPC	RW-MPC	
Negative Cut in (Case A)	0.60084	**0.34982**	**41.78 %**
Positive Cut in (Case B)	0.5558	**0.2042**	**63.26 %**
Cut out (Case C)	**0.1714**	0.1871	− 5.49 %

Table 5. Comparison of fuel consumption of CW-MPC and RW-MPC.

Case study	F (gram)		Improvement
	CW-MPC	RW-MPC	
Negative Cut in (Case A)	16.079	**11.896**	**26.02 %**
Positive Cut in (Case B)	29.243	**18.906**	**35.35 %**
Cut out (Case C)	10.289	**7.851**	**23.7 %**

6. CONCLUSION

In this paper, a novel spacing control law is successfully developed to improve the fuel economy and ride comfort, yielding a safe driving. This control law is design based on model predictive control with real-time weight tuning strategy as an upper-level controller in adaptive cruise control system, which computes an optimal desired acceleration. The proposed spacing control law can satisfy such control objectives as high fuel economy and ride comfort simultaneously during the TMs. The contribution of this research is summarized as follows:

(1) In order to improve the fuel economy during the TMs, a new compromised control method, which considers to establish safe inter-vehicle distance with zero relative velocity behind a preceding vehicle, is developed by the proposed spacing control law based on MPC. Due to the complexity of inter-vehicle statements during the TMs, a real-time weight tuning strategy is also designed and applied to the spacing control law, which calculates an optimal control command. So that the host vehicle can establish safe inter-vehicle distance smoothly, thus ensuring the improvement of ride comfort and fuel economy simultaneously, whereas the existing studies do not consider the vehicle safety, fuel consumption, ride comfort and time-varying issues at the same time.

(2) The performance of ACC system with the proposed spacing control law is simulated by MatLab/Simulink combined with the Carsim-based vehicle model. This method is not commonly found in the existing literature. This indicates that the results are more realistic due to considering the nonlinearity of longitudinal dynamics in the vehicle-following plant.

ACKNOWLEDGEMENT–This research is supported by the University of Macau Research Grant [grant numbers MYRG077(Y1-L2)FST13-WPK & MYRG2016-00212-FST] and the Science and Technology Development Fund of Macau SAR [grant number: 107/2013/A3].

REFERENCES

Ali, Z., Popov, A. A. and Charles, G. (2013). Model predictive control with constraints for a nonlinear adaptive cruise control vehicle model in transition manoeuvres. *Vehicle System Dynamics: Int. J. Vehicle Mechanics and Mobility* **51**, **6**, 943−963.

Baghwar, V., Garrard, W. L. and Rajamani, R. (2004). Model predictive control of transitional maneuvers for adaptive cruise control vehicles. *IEEE Trans. Vehicular Technology* **53**, **5**, 1573−1585.

Connolly, T. R. and Hedrick, J. K. (1999). Longitudinal transition maneuvers in an automated highway system. *J. Dynamic Systems, Measurement and Control* **121**, **3**, 471−478.

Drehmer, L. R. C., Casas, W. J. P. and Gomes, H. M. (2015). Parameters optimisation of a vehicle suspension system using a particle swarm optimisation algorithm. *Vehicle System Dynamics: Int. J. Vehicle Mechanics and Mobility* **53**, **4**, 449−474.

Fancher, P. and Bareket, Z. (1994). Evaluating headway control using range versus range-rate relationships. *Vehicle System Dynamics: Int. J. Vehicle Mechanics and Mobility* **23**, **1**, 575−596.

Goggia, T., Sorniotti, A., De Novellis, L., Ferrara, A., Gruber, P., Theunissen, J., Steenbeke, D., Knauder, B. and Zehetner, J. (2015). Integral sliding mode for the torque-vectoring control of fully electric vehicles: Theoretical design and experimental assessment. *IEEE Trans. Vehicular Technology* **64**, **5**, 1701−1715.

Ioannou, P. and Xu, Z. (1994). Throttle and brake control system for automatic vehicle following. *J. Intelligent Transportation Systems* **1**, **4**, 345−377.

Kamal, M., Murata, J. and Kawabe, T. (2009). Development of ecological driving system using model predictive control. *Proc. ICROS-SICE Int. Joint Conf.*, 3549−3554.

Kim, S., Tomizuka, M. and Cheng, K. H. (2010). Smooth motion control of the adaptive cruise control system with linear quadratic control with variable weights. *Proc. ASME 2010 Dynamic Systems and Control Conf.*, 879−886.

Kim, S. G., Tomizuka, M. and Cheng, K. H. (2012). Smooth motion control of the adaptive cruise control system by a virtual lead vehicle. *Int. J. Automotive*

Technology **13**, **1**, 77−85.
Kato, S., Tsugawa, S., Tokuda, K., Matsui, T. and Fujii, H. (2002). Vehicle control algorithms for cooperative driving with automated vehicles and intervehicle communications. *IEEE Trans. Intelligent Transportation Systems* **3**, **3**, 155−161.
Li, S. B., Li, K. Q., Rajamani, R. and Wang, J. Q. (2011). Model predictive multi-objective vehicular adaptive cruise control. *IEEE Trans. Control Systems Technology* **19**, **3**, 556−566.
Luo, L., Liu, H., Li, P. and Wang, H. (2010). Model predictive control for adaptive cruise control with multi-objectives: Comfort, fuel-economy, safety and car-following. *J. Zhejiang University-Science A* **11**, **3**, 191−201.
Li, S. E., Li, K. Q. and Wang, J. Q. (2013). Economy-oriented vehicle adaptive cruise control with coordinating multiple objectives function. *Vehicle System Dynamics: Int. J. Vehicle Mechanics and Mobility* **51**, **1**, 1−17.
Liang, C. Y. and Peng, H. (1999). Optimal adaptive cruise control with guaranteed string stability. *Vehicle System Dynamics: Int. J. Vehicle Mechanics and Mobility* **32**, **4-5**, 313−330.
Lee, M. H., Park, H. G., Lee, S. H., Yoon, K. S. and Lee, K. S. (2013). An adaptive cruise control system for autonomous vehicles. *Int. J. Precision Engineering and Manufacturing* **14**, **3**, 373−380.
Martinez, J. J. and Canudas-De-Wit, C. (2007). A safe longitudinal control for adaptive cruise control and stop-and-go scenarios. *IEEE Trans. Control Systems Technology* **15**, **2**, 246−258.
McDonough, K., Kolmanovsky, I., Filev, D., Yanakiev, D., Szwabowski, S. and Michelini, J. (2013). Stochastic dynamic programming control policies for fuel efficient vehicle following. *Proc. American Control Conf.*, 1350−1355.
McGehee, J. and Yoon, H. S. (2015). Optimal torque control of an integrated starter-generator using genetic algorithms. *Proc. Institution of Mechanical Engineers Part D: J. Automobile Engineering* **229**, **7**, 875−884.
Naus, G. J., Ploeg, J., Van de Molengraft, M. J. G., Heemels, W. P. M. H. and Steinbuch, M. (2010). Design and implementation of parameterized adaptive cruise control: An explicit model predictive control approach. *Control Engineering Practice* **18**, **8**, 882−892.
Rajamani, R. (2012). *Vehicle Dynamics and Control*. 2nd edn. Springer. New York, USA.
Rajamani, R., Choi, S. B., Law, B. K., Hedrick, J. K., Prohaska, R. and Kretz, P. (2000). Design and experimental implementation of longitudinal control for a platoon of automated vehicles. *J. Dynamic Systems, Measurement, and Control* **122**, **3**, 470−476.
Sheikholeslam, S. and Desoer, C. A. (1993). Longitudinal control of a platoon of vehicles with no communication of lead vehicle information: A system level study. *IEEE Trans. Vehicular Technology* **42**, **4**, 546−554.
Swaroop, D. and Hedrick, J. K. (1996). String stability of interconnected systems. *IEEE Trans. Automatic Control* **41**, **3**, 349−357.
Sun, M., Lewis, F. L. and Ge, S. S. (2004). Platoon-stable adaptive controller design. *Proc. IEEE Conf. Decision and Control*, 5481−5486.
Santhanakrishnan, K. and Rajamani, R. (2003). On spacing policies for highway vehicle automation. *IEEE Trans. Intelligent Transportation Systems* **4**, **4**, 198−204.
Shakouri, P. and Ordys, A. (2014). Nonlinear model predictive control approach in design of adaptive cruise control with automated switching to cruise control. *Control Engineering Practice*, **26**, 160−177.
Shakouri, P., Ordys, A. and Askari, M. R. (2012). Adaptive cruise control with stop&go function using the state-dependent nonlinear model predictive control approach. *ISA Trans*. **51**, **5**, 622−631.
Xiao, L. Y. and Gao, F. (2010). A comprehensive review of the development of adaptive cruise control systems. *Vehicle System Dynamics: Int. J. Vehicle Mechanics and Mobility* **48**, **10**, 1167−1192.
Yi, K. and Kwon, Y. D. (2001). Vehicle-to-vehicle distance and speed control using an electronic-vacuum booster. *JSAE Review* **22**, **4**, 403−412.

APPENDIX

$$\boldsymbol{S}_{\mathrm{x}} = \begin{bmatrix} CA \\ CA^2 + CA \\ \vdots \\ \vdots \\ \sum_{\mathrm{i}=1}^{\mathrm{p}} CA^{\mathrm{i}-1} \end{bmatrix}_{\mathrm{p}\times 1}, \boldsymbol{I} = \begin{bmatrix} I_{\mathrm{n_c}\times\mathrm{n_c}} \\ I_{\mathrm{n_c}\times\mathrm{n_c}} \\ \vdots \\ I_{\mathrm{n_c}\times\mathrm{n_c}} \end{bmatrix}_{\mathrm{p}\times 1}, \boldsymbol{S}_{\mathrm{d}} = \begin{bmatrix} CB_{\mathrm{d}} \\ CAB_{\mathrm{d}} + CB_{\mathrm{d}} \\ \vdots \\ \sum_{\mathrm{i}=1}^{\mathrm{p}} CA^{\mathrm{i}-1} B_d \end{bmatrix}_{\mathrm{p}\times 1}$$

$$\boldsymbol{S}_{\mathrm{u}} = \begin{bmatrix} CB_{\mathrm{u}} & 0 & \cdots & 0 \\ \sum_{\mathrm{i}=1}^{2} CA^{\mathrm{i}-1}B_{\mathrm{u}} & CB_{\mathrm{u}} & \cdots & 0 \\ \vdots & \vdots & \vdots & \vdots \\ \sum_{\mathrm{i}=1}^{\mathrm{m}} CA^{\mathrm{i}-1}B_{\mathrm{u}} & \sum_{\mathrm{i}=1}^{\mathrm{m}} CA^{\mathrm{i}-1}B_{\mathrm{u}} & \cdots & CB_{\mathrm{u}} \\ \vdots & \vdots & \vdots & \vdots \\ \sum_{\mathrm{i}=1}^{\mathrm{p}} CA^{\mathrm{i}-1}B_{\mathrm{u}} & \sum_{\mathrm{i}=1}^{\mathrm{p}-1} CA^{\mathrm{i}-1}B_{\mathrm{u}} & \cdots & \sum_{\mathrm{i}=1}^{\mathrm{p}-\mathrm{m}+1} CA^{\mathrm{i}-1}B_{\mathrm{u}} \end{bmatrix}_{\mathrm{p}\times\mathrm{m}}$$

$$C_{\mathrm{u}} = \begin{bmatrix} -\boldsymbol{T}^{\mathrm{T}} & \boldsymbol{T}^{\mathrm{T}} & -\boldsymbol{L}^{\mathrm{T}} & \boldsymbol{L}^{\mathrm{T}} & -\boldsymbol{S}_{\mathrm{u}}^{\ \mathrm{T}} & \boldsymbol{S}_{\mathrm{u}}^{\ \mathrm{T}} \end{bmatrix}_{(4\mathrm{m}+2\mathrm{p})\times 1}$$

$$b(k+1|k)=\begin{bmatrix} -\Delta u_{max}(k) \\ \vdots \\ -\Delta u_{max}(k+m-1) \\ \Delta u_{min}(k) \\ \vdots \\ -\Delta u_{min}(k+m-1) \\ u(k-1)-u_{max}(k) \\ \vdots \\ u(k-1)-u_{max}(k+m-1) \\ \Delta u_{min}(k)-u(k-1) \\ \vdots \\ \Delta u_{min}(k+m-1)-u(k-1) \\ Y_p(k+1|k)-Y_{max}(k+1) \\ Y_p(k+1|k)+Y_{min}(k+1) \end{bmatrix}_{(4m+2p)\times 1}$$